Available online at www.sciencedirect.com
SCIENCE DIRECT®
Nuclear Physics B (Proc. Suppl.) 151 (2006) 393–400
NUCLEAR PHYSICS B PROCEEDINGS SUPPLEMENTS
www.elsevierphysics.com

The Pierre Auger Observatory – status and prospects

Karl-Heinz Kampert[a] * for the Pierre Auger Collaboration[†]

[a] Bergische Universität Wuppertal, Fachbereich C - Physik, 42097 Wuppertal, Germany

The southern Pierre Auger Observatory is presently under construction in Malargüe, Mendoza, Argentina. It combines two complementary air shower observation techniques; the detection of particles at ground and the observation of associated fluorescence light generated in the atmosphere above the ground. Experimentally, this is being realized by employing an array of 1600 water Cherenkov detectors, distributed over an area of 3000 km^2, and operating 24 wide-angle Schmidt telescopes, positioned at four sites at the border of the ground array. The Observatory will reach its full size in 2006. However, with the 540 tanks and 12 telescopes presently in operation, the Pierre Auger Observatory has become already now the world-wide largest cosmic ray experiment. This paper sketches the experimental set-up and discusses the current status. In parallel to the ongoing completion of the experiment, a large number of events have been detected with energies above 10^{19} eV. The data are used to verify both the performance of the individual detector components as well as to test the quality of the hybrid event reconstruction. All results obtained so far are very promising and they underline the great advantages of the chosen hybrid approach.

1. Introduction

Over the past decade, interest in the nature and origin of extremely high energy cosmic rays (EHECR) has grown enormously. Of particular interest are cosmic rays with energies $\geq 10^{20}$ eV. There is a twofold motivation for studying this energy regime, one coming from particle physics because cosmic rays give access to elementary interactions at energies much higher than man-made accelerators can reach, and another coming from astrophysics, because we do not know what kind of particles they are and where and how they acquire such enormous energies. An excellent review, published by Michael Hillas 20 years ago [1], presented the basic requirements for particle acceleration to energies $\geq 10^{19}$ eV by astrophysical objects. The requirements are not easily met, which has stimulated the production of a large number of creative papers.

The problem is aggravated even more by the fact that at these energies protons and nuclei should interact with the Cosmic Microwave Background (CMB). Above a threshold energy of $E_{\rm GZK} \simeq 5 \times 10^{19}$ eV protons lose their energy over relatively short cosmological distances via photo-pion production $p + \gamma_{\rm CMB} \rightarrow \pi^0 + p$ or $\pi^+ + n$. Iron nuclei get degraded at similar energies through photo-dissociation in the giant nuclear resonance regime, Fe$+\gamma_{\rm CMB} \rightarrow X + n$. Photons interact even more rapidly with the CMB by producing e^+e^--pairs. Thus, particles that have traveled over distances of 50 or 100 Mpc are unlikely to retain an energy of $\sim 10^{20}$ eV or more when they reach us. This was already recognized in the 1960's shortly after the discovery of the CMB and is called the Greisen-Zatsepin-Kuzmin (GZK) cutoff [2] (see also opening remarks of Prof. Zatsepin at this conference). Thus, not only do we not know how particles could obtain such extreme energies even in the most powerful astrophysical accelerators, these accelerators have to be located nearby on cosmological scales!

To solve this most pressing puzzle of high energy astroparticle physics, one either needs to invent nearby exotic EHECR sources or find ways of evading the GZK effect. Top-Down models with decaying topological defects or decaying superheavy relic particles are typical representatives of the former group. While typical representatives

*email: kampert@uni-wuppertal.de
[†]Observatorio Pierre Auger, Av. San Martín Norte 304, (5613) Malargüe, Argentina

0920-5632/$ – see front matter
doi:10.1016/j.nuclphysbps.2005.07.038

of the latter are violation of the Lorentz invariance, propagation of heavy supersymmetric particles, or the Z-burst model. A comprehensive review, with emphasis placed on top-down models, is given by Ref. [3]. Generally, the top-down models predict a dominance of photons and neutrinos over protons or nuclei, so that measurements of the chemical composition become important also at the highest energies. Furthermore, the Z-burst model cannot avoid producing a strong background of GeV energy photons leading to severe constrains due to the measured EGRET fluxes [4]. Such complications have recently given more emphasis again to astrophysical sources.

While the large magnetic rigidity of $\sim 10^{20}$ eV protons gives rise to the problems of particle acceleration in astrophysical sources, it opens at the same time a new window for astronomy with cosmic rays. Since such particles cannot be much deflected in the magnetic fields of the Galaxy and in extragalactic space, they should point to their sources within a few degrees deviation only. For example, using nominal guesses of 1 nG for the magnetic field strength of extragalactic space and 1 Mpc for the coherence length, deviations for protons on the order of 2.5° are expected after traveling 50 Mpc [5].

Two types of experiments based on very different techniques have undoubtedly detected particles well exceeding the GZK cut-off [6–8]. Unfortunately, despite 40 years of data taking the number of events is still small. Also, the largest experiments so far disagree at an approx. 2σ level on the flux and on arrival direction correlations. The HiRes collaboration, employing the fluorescence technique, claims to detect a suppression of the flux above the GZK-threshold, with no evidence for clustering in the arrival directions [8,9]. On the other hand, ground arrays have detected no GZK-cutoff [6,7]. Furthermore, the AGASA collaboration claims to see a clustering of the highest energy events [7] which, however, is not free of dispute [10]. Clearly, the situation is very puzzling, and a larger sample of high quality data is needed for the field to advance.

2. The Pierre Auger Observatory

Years before the present controversy between different experiments started, it was already clear that not only a much larger experiment was needed to improve the statistics of EHECRs on reasonable time scales but also that two or more complementary experimental approaches had to be combined on a shower-by-shower basis within one experiment. Such redundancy allows cross-correlations between experimental techniques, thereby controlling the systematic uncertainties. Furthermore, one expects to improve the resolution of the energy, mass, and direction of reconstructed primary particles. In the Pierre Auger Observatory, this so-called 'hybrid' aspect is realized by combining a ground array of water Cherenkov detectors with a set of fluorescence telescopes. Another important objective was to obtain a uniform exposure over the full sky. This will be achieved by constructing two instruments, each located at mid-latitudes in the southern and northern hemispheres. Each site is conceived to cover an area of 3000 km^2 in order to collect about 1 event per week and site above 10^{20} eV.

The Auger collaboration has started construction of the southern site in Malargüe, located at an elevation of 1400 m in the Province of Mendoza, Argentina. After successful operation of a prototype experiment (engineering array) [11], the southern observatory is now in full construction, to be completed in 2006. The northern observatory is planned to be sited in the U.S., either in Utah or Colorado.

2.1. Surface detector

The ground array will comprise 1600 cylindrical water Cherenkov tanks of 10 m^2 surface area and 1.2 m height (see Fig. 1). The tanks are arranged on a hexagonal grid with a spacing of 1.5 km yielding full efficiency for extensive air shower (EAS) detection above $\sim 5 \cdot 10^{18}$ eV. The water in the tanks is produced by a water plant at the observatory campus and its quality is about 15 MΩ·cm. The Cherenkov light produced by traversing muons, electrons, and converted photons is reflected inside the tank by a

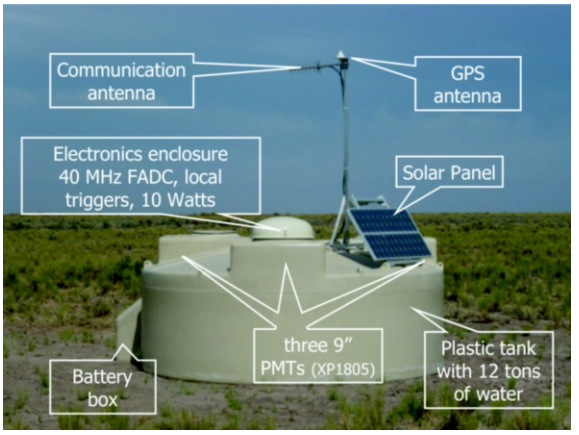

Figure 1. Photograph of a typical water tank in the Pampa Amarilla. The main components are indicated.

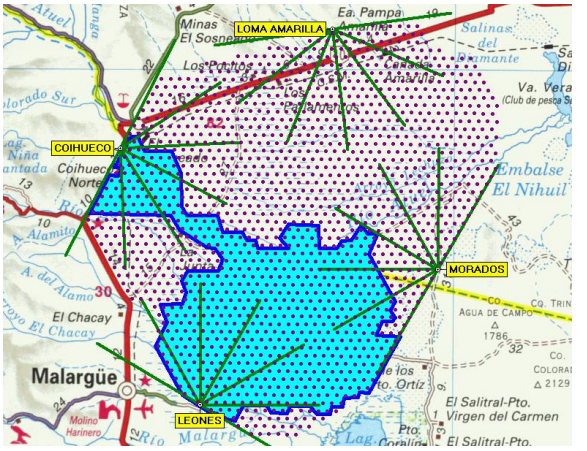

Figure 2. Layout of the southern site with the locations of the SD tanks indicated. Also shown are the locations of the FD-eyes with the f.o.v. of their telescopes. The grey region indicates the part of the SD currently in operation. Furthermore, all telescopes at the Los Leones and Coihueco sites are in operation since July 2004.

white diffusive Tyvec® liner and is detected by three 9" XP1805 Photonis photomultiplier tubes (PMTs). The PMT signals from the last dynode and the anode are continuously sampled at 40 MHz by six 10-bit FADCs, yielding a dynamic signal range in total of 15 bits. The digitized data are stored in ring buffer memories and processed by a programmable logic device (FPGA) to implement various trigger conditions [12,13]. Two solar panels, combined with buffer batteries, provide the electric power for the local electronics, for the GPS clock, used for absolute timing, and for the bi-directional radio communication. Recorded signals are transferred to the Central Data Acquisition System (CDAS) only in cases where a shower trigger has been detected in 3 adjacent tanks simultaneously.

The water tanks of the surface detector (SD) are continuously monitored and calibrated by single cosmic muons. By adjusting the trigger rates, the PMT gains are matched to within 5 %. For convenience, the number of particles in each tank is defined in units of Vertical Equivalent Muons (VEM), which is the average charge signal produced by a penetrating down going muon in the vertical direction. The stability of the continuously monitored tanks is very high and the trigger rates are remarkably uniform over all detector stations [13].

2.2. Fluorescence detector

Charged particles propagating through the atmosphere excite nitrogen molecules causing the emission of (mostly) ultraviolet light. The fluorescence yield is very low, approx. 4 photons per meter of electron track (see e.g. [14]), but can be measured with large area imaging telescopes during clear new- to half-moon nights (duty cycle of $\approx$ 10-15 %). The fluorescence detector (FD) of the southern site will comprise 24 telescopes arranged into 4 'eyes' located at the perimeter of the SD. The eyes are situated at locations which are slightly elevated with respect to the ground array. Each eye houses 6 Schmidt telescopes with a $30^\circ \times 30^\circ$ field of view (f.o.v.). Thus, the 6 telescopes of an eye provide a 180° view towards the array centre and they look upwards from 1° to 31° above the horizon. The layout of the southern site is is depicted in Fig. 2 and shows the locations of telescopes and water tanks already in operation. Figure 3 shows a photograph of a tele-

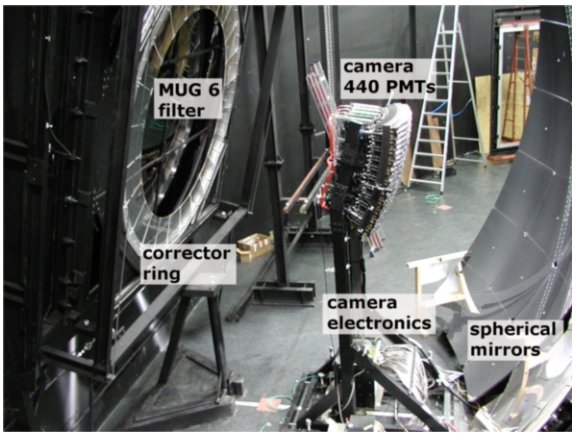

Figure 3. Photo of a FD telescope with its major elements indicated.

scope as taken during the installation. The main elements of the aperture system are the 2.2 m diaphragm including a corrector ring (not installed at each telescope, yet) and an UV transmission filter made of MUG-6 glass. The light is reflected by segmented 13 m^2 spherical mirrors. Because of limited production capacity, two types of mirror elements are used in different telescopes; either 49 hexagonal shaped glass mirrors or 36 rectangular shaped aluminum mirrors. The focal plane of the mirror is instrumented with a camera arranged in 20×22 pixels. Thus, each of the 440 PMTs (XP 3062 of Photonis) of a camera views approximately $1.5° \times 1.5°$ of the sky. The PMT signals are continuously digitized at 10 MHz sampling rate with a dynamic range of 15 bit in total. An FPGA based multi-level trigger system records traces out of a random background of 100 Hz per pixel [15].

To determine the shower energies correctly, accurate measurements and monitoring of the PMT gains is needed. This is primarily accomplished by a diffuse surface which is mounted for calibration purposes outside the telescope building in front of the telescope aperture to uniformly illuminate the telescope f.o.v. with a calibrated light signal [16]. Furthermore, the attenuation of the light from the EAS to the telescope due to molecular (Rayleigh) and aerosol scattering has to be corrected for. The relevant parameters are determined by a Horizontal Attenuation Monitor (HAM), Aerosol Phase Function monitors (APF) and LIDAR systems located at each of the eyes [17].

3. First results

The southern observatory has presently (Nov. 2004) more than 540 tanks and two complete FD eyes (Los Leones and Coihueco, each with 6 telescopes) fully operational and taking data. With about 1000 km^2 covered by the ground array and 1500 km^2 observed by the FD, the Auger Observatory has become the largest and most complete cosmic ray detector in the world. A large number of events with ever increasing rate is continuously being collected and analyzed by many different groups.

3.1. First events in the SD

Figure 4 shows some typical examples of EAS footprints as seen by the SD. The diameter of the circles indicates the particle densities (VEMs) detected in the respective tanks. The shower direction is determined by a plane fit to the shower front as determined from the particle arrival times. The energy and core position is reconstructed by performing a fit of a lateral distribution function (LDF) to the number of VEMs seen by the different tanks. As an example, Fig. 5 depicts the reconstructed LDF for the EAS of Fig. 4(b); the richness and quality of the data is evident. EAS simulations have shown that the primary energy, in the considered range, is best determined from the value of the LDF at a distance of 1000 m from the shower core. This number, generally named $S(1000)$, is found to be the least affected by fluctuations caused by both the longitudinal shower development and by the unknown mass of the primary particle.

Besides the particle densities reconstructed from the integrated signals in the water tanks, rich information is also contained in the time traces of the recorded signals. These allow the identification of narrow spikes from individual muons at distances beyond a few 100 m from the shower core so that appropriate filtering tech-

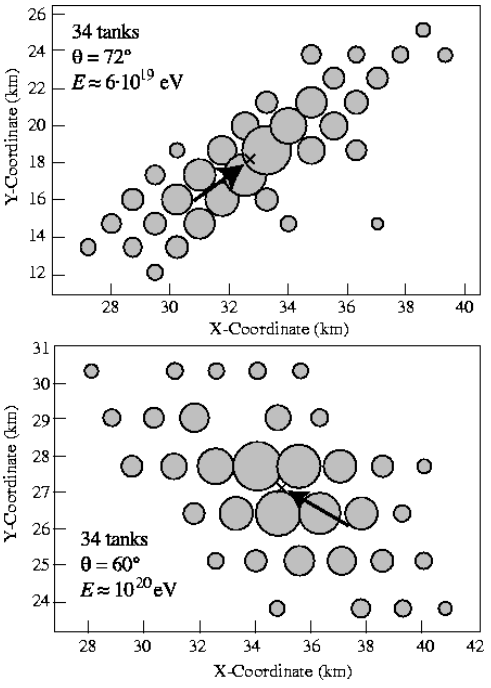

Figure 4. Example of two EAS as seen by the SD; the size of the circles represents the particle densities measured in the water tanks, the directions and shower core positions are indicated by the arrows and ×-symbols.

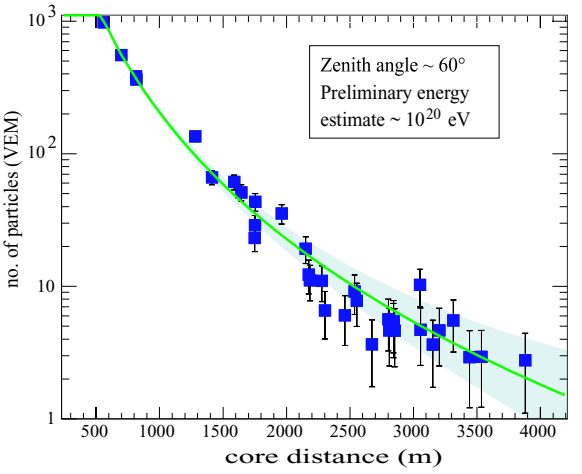

Figure 5. Reconstructed lateral distribution function of the 10^{20} eV EAS of Fig. 4(b).

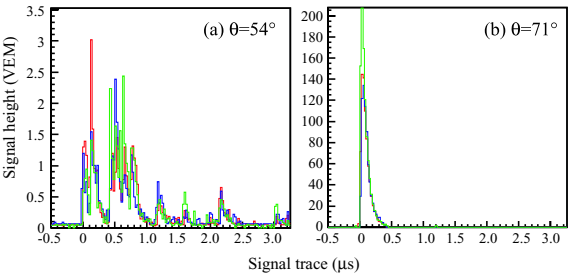

Figure 6. Typical signal traces as recorded by the FADC system for detectors at about 800 m from the shower core. The narrow time profiles seen in (b) are characteristic for very inclined showers induced by hadrons. The different colors (grey-scales) represent the signals of the individual PMTs within a detector.

niques enable electron-muon separation, in turn providing information about the primary mass. Furthermore, in very inclined EAS ($\Theta \gtrsim 75°$), the electromagnetic and soft muonic components get almost completely absorbed during the propagation through the atmosphere; only hard muons with a very narrow time profile and small shower front curvature can reach the detectors. Vertical showers, on the contrary, do contain many electrons spread over several μs in time. These distinct differences in the time structures are easily seen in Fig. 6 and they open a window to neutrino astronomy in the EeV region. This is because a horizontal EAS, showing the timing characteristics of a ("young") non-horizontal EAS, can only be initiated by a neutrino interacting close to the ground array. Simulations show that this signature allows almost background free neutrino detection. This feature, combined with the large acceptance of the water Cherenkov tanks to horizontally propagating particles, provides a neutrino sensitivity, which allows the testing of various AGN and top-down models [18]. Calculations of the Auger acceptance to showers produced by Earth skimming tau neutrinos have also been made. Again, it turns out that the results are very encouraging [19].

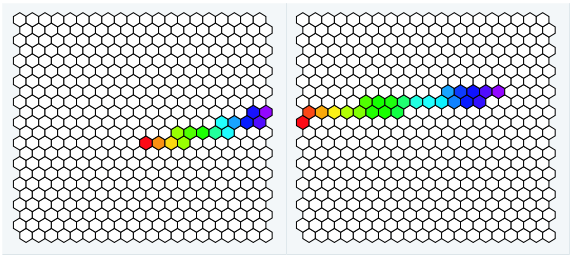

Figure 7. Light track of a hybrid event as seen by two adjacent fluorescence cameras. The zenith angle is $\theta = 71°$ and the nearest distance of the EAS to the telescopes is about 20.5 km. The different colors (grey-scales) indicate the time progression of the pixels in the respective cameras. Other traces of the same event are shown in Figs. 6(b), 9, and 10.

3.2. First events in the FD and aspects of hybrid reconstruction

In the fluorescence detector, cosmic ray showers are seen as a sequence of triggered pixels in the camera. An example of an event propagating through two adjacent telescopes is presented in Fig. 7. The first step in the analysis is the determination of the shower detector plane (SDP) reconstructed from the viewing direction of the PMT pixels (see illustration in Fig. 8). Next, the timing information of the pixels is used for reconstructing the shower axis within the SDP. For a given geometry, the arrival time t_i of light at a pixel i is given by

$$t_i = t_0 + \frac{R_p}{c} \cdot \tan[(\chi_0 - \chi_i)/2].$$

c denotes the speed of light and t_0, R_p, and χ_0 are fit parameters as illustrated in Fig. 8. As an example, Fig. 9 shows the time vs. angle correlation for the event shown in Fig. 7. It is clear that the uncertainty of the three parameters depends on the particular geometry and on the observed track length. For short tracks there may be only insignificant curvature in the tangent function of the above expression so that an ambiguity remains in the family of possible (R_p, χ_0) solutions. This translates directly into an uncertainty in the reconstructed shower energy be-

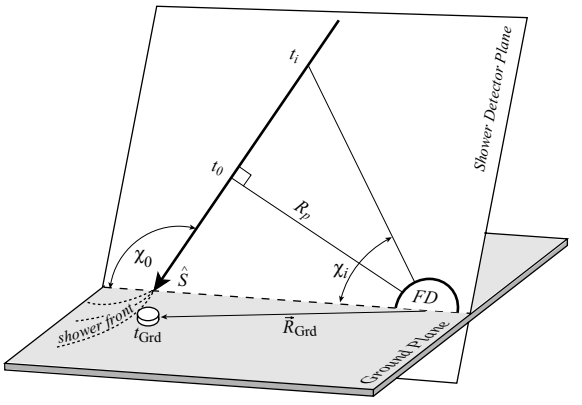

Figure 8. Illustration of the geometrical shower reconstruction from the observables of the fluorescence telescopes.

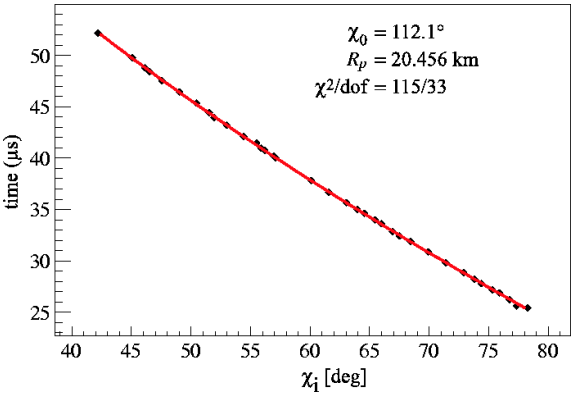

Figure 9. Time vs angle correlation for the hybrid event shown also in Figs. 6(b) and 7; the fit parameters are also given in the figure.

cause $E_{\rm prim.} \propto L_{\rm fluor.} \propto L_{FD} \cdot R_p^2 \cdot \exp(R_p/\lambda_{\rm att})$ with $\lambda_{\rm att}$ being the effective attenuation length of fluorescence light. This asymmetric uncertainty in the energy reconstruction and the asymmetric angular resolution are important drawbacks of a fluorescence detector used in the so called mono-reconstruction mode.

One way to improve the situation is provided by stereo observations of EAS. With all 4 FD eyes in operation, the Pierre Auger Observatory will achieve full efficiency for stereo observation

at energies above $\sim 2 \cdot 10^{19}$ eV. Another very effective way to improve shower reconstruction and to break the aforementioned ambiguities in the (R_p, χ_0)-plane is accomplished by combining the information of the surface array with that of the fluorescence telescopes. This is called the hybrid reconstruction and is even effective for low energy showers. As illustrated in Fig. 8, the timing information (and location constraint) from a hit ground array station $t_{\rm GND}$ can be related to the time t_0 at which the shower reaches the position of closest approach to the telescope:

$$t_0 = t_{\rm GND} - (\vec{R}_{\rm GND} \cdot \hat{S})/c.$$

Here, $\vec{R}_{\rm GND}$ denotes the direction of the hit ground station and $\hat{S}$ is the unit vector of the shower axis (see Fig. 8).

Since the SD operates at a 100 % duty cycle, most of the events observed by the FD are in fact hybrid events with the exception only at low energies. Even without full reconstruction of the EAS by the ground array, the timing information of a single tank provides sufficient information for the hybrid reconstruction.

In such analyses the time synchronization between different detector components is very important, particularly between the fluorescence telescopes and the ground array. To verify this and to test the reconstruction procedure outlined above, artificial events have been generated by the central laser facility (CLF). At a distance of about 26 km from the telescopes, laser shots have been directed vertically towards the sky and a small portion of the light has been fed into a water tank nearby by using a light fiber. In such a way, the 'shower' axis of the laser light could be reconstructed both in mono-mode and in the single-tank hybrid mode. The results are very convincing; in mono reconstruction the location of the CLF could be determined with a resolution of 550 m and after including the timing information of the single water tank, the resolution improved to 20 m with no systematic shift!

After successful reconstruction of the event geometry, the FADC signals of the FD-pixels are analyzed in order to obtain the light emitted along the shower axis. This step of the analysis uses an atmospheric scattering model to transform the light received at the detector back to the light emitted from the shower axis. Also, the geometrical height as observed by the telescope pixels is converted to grammage of atmosphere, being more relevant for the shower development [21,22]. The amount of fluorescence light emitted from a volume of air is proportional to the energy dissipated by the shower particles in that volume. Therefore, the observed longitudinal light profile represents the energy loss in the atmosphere which in turn is highly proportional to the number of charged particles in a given volume. The result for the hybrid shower, shown in Figs. 6(b), 7, and 9, is presented in Fig. 10; again, the quality of data is evident. The line represents the best fit Gaisser-Hillas function [20] yielding a primary energy in agreement with the $S(1000)$ determination.

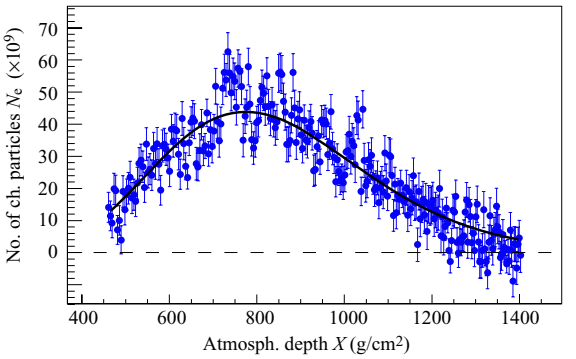

Figure 10. Longitudinal shower profile of the hybrid event shown also in Figs. 6b, 7, and 9. The line represents the result of a Gaisser-Hillas fit [20].

Several hundred good quality hybrid events have been collected so far and their number is progressively increasing because of progress in the installation of tanks and telescopes. Preliminary analyses of the hybrid data show good consistency between the energy estimates of the SD and FD.

4. Summary and outlook

The construction of the southern Pierre Auger Observatory is well underway. Half of the telescopes and about a third of the surface array are

in operation and are taking data routinely. If the present rate of deployment is maintained, being currently limited only by funding, construction will be finished in 2006. The detectors are performing very well and data analysis has begun. Besides reconstructing events from the SD and FD individually, and comparing their results on a shower-by-shower basis, emphasis is placed on hybrid analyses providing unprecedented quality in geometry, energy, and mass reconstruction. Of primary importance for the near future will be the determination of the energy spectrum to study the GZK effect and to search for anisotropies in arrival direction. The detection of very inclined showers enables clear and almost background free measurements of ultra-high energy neutrinos. The aperture is sufficient to verify or exclude a number of models discussed in the literature.

In parallel to the completion of the southern observatory and to the analysis of data towards first science results, R&D has started for the development of the northern site.

Acknowledgement: It is a pleasure to thank the organizers of the Symposium for their invitation to participate in a very interesting and fruitful meeting conducted in a pleasant atmosphere. The work of the group at University Wuppertal is supported in part by the German Ministry for Research and Education (Grant 05 CU1VK1/9).

REFERENCES

1. M. Hillas, *Ann. Rev. Astron. Astrophys.* **22** (1984) 425.
2. K. Greisen, *Phys. Rev. Lett.* **16** (1966) 748; G.T. Zatsepin and V.A. Kuz'min, *Sov. Phys. JETP Lett.* (Engl. Transl.), **4** (1966) 78.
3. P. Bhattacharjee and G. Sigl *Phys. Rep.* **327** (2000) 109.
4. G. Sigl, *Acta Phys. Polon.* **B35** (2004) 1845.
5. J.W. Cronin, *Nucl. Phys. (Proc. Suppl.)* **B28** (1992) 1992.
6. M. Nagano and A.A. Watson, *Rev. Mod. Phys.* **72** (2000) 869.
7. M. Takeda et al. (AGASA-Collaboration), *Astropart. Phys.* **19** (2003) 135.
8. R.U. Abbasi et al. (HiRes-Collaboration), *Phys. Rev. Lett.* **92** (2004) 151101; *Astropart. Phys.* **22** (2004) 139.
9. R.U. Abbasi et al. (HiRes-Collaboration), *Astrophys. J.* **610** (2004) L73.
10. C.B. Finley and S. Westerhoff, *Astropart. Phys.* **21** (2004) 359.
11. J. Abraham et al. (Auger Collaboration), *Nucl. Instr. Meth.* **A523** (2004) 50.
12. Z. Szadkowski and D. Nitz, subm. to *Nucl. Instr. Meth.* (2004).
13. T. Suomijarvi et al. (Auger Collaboration), *Nucl. Phys. B (Proc. Suppl.)* **136** (2004) 393.
14. F. Kakimoto et al., *Nucl. Instr. Meth. A* **372** (1996) 527.
15. M. Kleifges et al. (Auger Collaboration), *Nucl. Instr. Meth. A* **518** (2004) 180.
16. M.D. Roberts et al. (Auger Collaboration), *28th ICRC (Tsukuba)* **1**, (2003), 453.
17. M.A. Mostafa et al. (Auger Collaboration), *28th ICRC (Tsukuba)* **1**, (2003), 465.
18. K.S. Capelle et al., *Astropart. Phys.* **8** (1998) 321.
19. X. Bertou et al., *Astropart. Phys.* **17** (2002) 183.
20. T.K. Gaisser and A.M. Hillas, *Proceedings of the 15th International Cosmic Ray Conference* **8** (1977) 353.
21. P. Privitera et al. (Auger Collaboration), *Nucl. Phys. B (Proc. Suppl.)* **136** (2004) 399.
22. L. Perrone et al. (Auger Collaboration), *Nucl. Phys. B (Proc. Suppl.)* **136** (2004) 407.